ACS APPLIED MATERIALS & INTERFACES

Research Article

www.acsami.org

Highly Efficient Blue–Green Quantum Dot Light-Emitting Diodes Using Stable Low-Cadmium Quaternary-Alloy ZnCdSSe/ZnS Core/Shell Nanocrystals

Huaibin Shen,[†,§] Sheng Wang,[†,§] Hongzhe Wang,[†] Jinzhong Niu,[†] Lei Qian,[†] Yixing Yang,[‡] Alexandre Titov,[‡] Jake Hyvonen,[‡] Ying Zheng,*[,‡] and Lin Song Li*[,†]

[†]Key Laboratory for Special Functional Materials, Henan University, Kaifeng 475004, P. R. China

[‡]NanoPhotonica Inc., 747 SW Second Avenue, Gainesville, Florida 32601, United States

Supporting Information

ABSTRACT: High-quality blue–green emitting $Zn_xCd_{1-x}S_{1-y}Se_y$/ZnS core/shell quantum dots (QDs) have been synthesized by a phosphine-free method. The quantum yields of as-synthesized $Zn_xCd_{1-x}S_{1-y}Se_y$/ZnS core/shell QDs can reach 50–75% with emissions between 450 and 550 nm. The emissions of such core/shell QDs are not susceptible to ligand loss through the photostability test. Blue-green light-emitting diodes (LEDs) based on the low-cadmium $Zn_xCd_{1-x}S_{1-y}Se_y$/ZnS core/shell QDs have been successfully demonstrated. Composite films of poly[9,9-dioctylfluorene-co-*N*-[4-(3-methylpropyl)]-diphenylamine] (TFB) and ZnO nanoparticle layers were chosen as the hole-transporting and the electron-transporting layers, respectively. Highly bright blue–green QD-based light-emitting devices (QD-LEDs) showing maximum luminance up to 10000 cd/m^2, in particular, the blue QD-LEDs show an unprecedentedly high brightness over 4700 cd/m^2 and peak external quantum efficiency (EQE) of 0.8%, which is the highest value ever reported. These results signify a remarkable progress in QD-LEDs and offer a practicable platform for the realization of QD-based blue–green display and lighting.

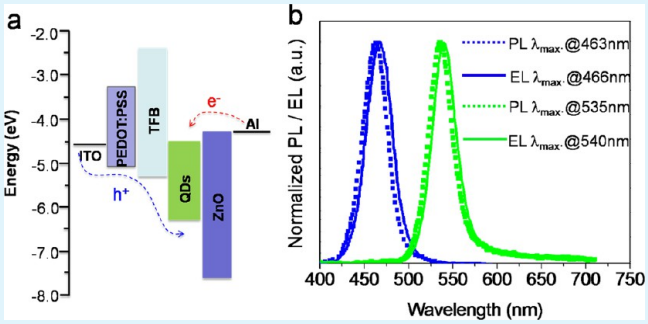

KEYWORDS: *ZnCdSSe/ZnS, alloy, core/shell, blue–green, QD-LEDs, electroluminescence*

INTRODUCTION

Semiconductor quantum dots (QDs) show great promise for use in QD-based light-emitting devices (QD-LEDs), displays, and other photoelectric devices owing to their unique optical properties.[1−17] It is well-known that the tuning of photoluminescence (PL) emission is accessible through altering the size of the particles for binary II–VI QDs such as CdS and CdSe which have been most intensively investigated.[18] However, these binary QD systems are still not very easy to deliver high quantum yield (QY) and stable blue–green emission between 450 and 530 nm due to the unstable fine particles are difficult to passivate by overcoating shells. However, the wavelength at 450 and 530 nm are of particular interest for the preparation of QD-based blue–green LEDs and as "must-have" emitters for next-generation displays and white solid-state lighting. Therefore, it is still very important to exploit new synthesis methods since the efficient and controllable synthesis of high quality blue–green QDs is still a challenging topic. Recently, alloyed $Zn_{1-x}Cd_x$ based chalcogenide QDs (such as $Zn_{1-x}Cd_xS$, $Zn_{1-x}Cd_xSe$ and $Zn_xCd_{1-x}S_ySe_{1-y}$)[19−25] have arisen as attractive candidates because their composition sensitive emissions can be easily tuned to cover the whole visible range and high operability for subsequent stability enhancement processes. Those alloyed QDs are high potential materials for stable and high performance blue emitters which may surpass the drawbacks of binary QD emitters.

In this paper, we have prepared high-quality blue–green emitting quaternary ZnCdSSe QDs, which adjusted the optical performance by not only the radio between Zn and Cd but also the radio between Se and S and the PL QYs could reach up to 40%. To improve the QY and stability of ZnCdSSe QDs, high-quality blue–green emitting low-cadium ZnCdSSe/ZnS core/shell QDs have been synthesized by a phosphine-free method. The QYs of as-synthesized ZnCdSSe/ZnS core/shell QDs can reach 50–75% with emissions between 450 and 550 nm. We also demonstrated blue–green light-emitting diodes based on the ZnCdSSe/ZnS core/shell QDs. The highly bright blue–green QD-LEDs show a peak luminance up to 10000 cd/m^2. In particular, the blue QD-LEDs show unprecedentedly high brightness over 4700 cd/m^2, which is the highest value ever reported and indicates the ZnCdSSe/ZnS core/shell QDs are more suitable for making blue QD-LEDs. These results provide

Received: January 31, 2013
Accepted: April 30, 2013
Published: April 30, 2013

reliable conveniences for the realization of QD-based full color displays and lighting devices.

EXPERIMENTAL DETAILS

Chemicals. All reagents were used as received without further experimental purification. Zinc oxide (ZnO, 99.99% powder), cadmium oxide (CdO, 99.99%, powder), sulfur (S, 99.98%, powder), 1-octadecene (ODE, 90%), oleic acid (OA, 90%), decanoic acid (99%), and selenium (Se, 99.99%, powder) were purchased from Aldrich. Hexanes (analytical grade), paraffin oil (analytical grade), and methanol (analytical grade) were obtained from Beijing Chemical Reagent Ltd., China.

Preparation of precursors. *Stock Solution for Zn−Cd Precursor.* A mixture (30 mL in total) of CdO (0.5760 g, 4.5 mmol) and ZnO (0.3645 g, 4.5 mmol), oleic acid (27 mmol, 9 mL), and 21 mL paraffin oil was loaded in a 50 mL three-neck flask and heated to 260 °C under nitrogen to obtain a colorless clear solution. The resulting solution was allowed to cool down to 100 °C for injection.

Stock Solution for Zn Precursor. A mixture (30 mL in total) of ZnO (0.2441 g, 3 mmol), oleic acid (25 mmol, 8 mL), and 22 mL paraffin oil was loaded in a 50 mL three-neck flask and heated to 310 °C under nitrogen to obtain a colorless clear solution. The resulting solution was allowed to cool down to 130 °C for shell growth.

Stock Solution for S Precursor. The sulfur precursor solution (0.1 M) was prepared by dissolving sulfur (0.064 g, 2 mmol) in ODE (20 mL) at 150 °C.

Synthesis of $Zn_{0.5}Cd_{0.5}S_{0.25}Se_{0.75}$ QD. QDs with various ratios of Zn to Cd and S to Se have been synthetized. The $Zn_{0.5}Cd_{0.5}S_{0.25}Se_{0.75}$ QD was used as an example. A 0.1 mmol portion of S and 0.3 mmol of Se were mixed with 15 mL paraffin liquid, degassed for 30 min, filled with N_2, and heated to 310 °C. At this temperature, 3 mL of $Zn_{0.5}Cd_{0.5}$ precursor solution was quickly injected to the flask containing the above mixture. The new mixture was then maintained at 260 °C under continuous stirring. Aliquots were taken at different time intervals such as 10 s, 1 min, 5 min, and 30 min, respectively. The as-synthesized QDs were purified by repeated precipitation with methanol and redispersed in hexanes for several times. Other types of $Zn_{1-x}Cd_xS_{1-y}Se_y$ QDs were prepared and purified following the same procedures as described above for $Zn_{0.5}Cd_{0.5}S_{0.25}Se_{0.75}$ QDs. The ratio of S to Se and Zn to Cd varied from 7:1 to 1:7 and 8:1 to 1:8, respectively.

Synthesis of $Zn_{1-x}Cd_xS_{1-y}Se_y$/ZnS Core/Shell QDs with Blue−Green Emission. It is well-known that the lattice mismatch between the core and shell seriously limits the PL intensity. One solution is to use a core and multishell structure such as CdSe/CdS/CdZnS/ZnS.[26] But this route is complex because of too many precursors. The lattice mismatch between the $Zn_{1-x}Cd_xS_{1-y}Se_y$ core and ZnS shell is relatively small so that this core/shell NCs structure not only simplifies the synthesis process but also improves the QYs. The growth of ZnS shells was performed by the method reported previously.[27] A typical synthesis was performed as follows: 4 mL of ODE and 3 g of ODA were loaded into a 100 mL reaction vessel. The purified $Zn_{1-x}Cd_xS_{1-y}Se_y$ QDs in hexanes (3.5 nm in diameter, 3×10^{-7} mol) were added, and the system was kept at 100 °C under N_2-flow for 30 min to remove the hexanes and other undesired materials of low vapor pressure. Subsequently, the solution was heated up to 300 °C under N_2-flow where the shell growth was performed. This is followed by alternating addition of Zn precursor and S-ODE precursor, respectively, and the amount of which were calculated from the respective volumes of concentric spherical shells with a thickness of one hypothetical monolayer. An interval of 20 min was set for the growth of S layers and an interval of 30 min was set for the growth of Zn layers. Finally, a small amount of hexanes was added into the QDs solution and the unreacted compounds and byproducts were removed by successive methanol extraction (at least three times).

Fabrication and Characterization of QD-LED. ZnO nanoparticles were synthesized by a solution-precipitation process using Zn acetate and tetramethylammonium hydroxide (TMAH).[11] For a typical synthesis, a solution of zinc acetate in dimethyl sulphoxide (DMSO) (0.5 M) and 30 mL of a solution of TMAH in ethanol (0.55 M) were mixed and stirred for 1 h in ambient air, then washed and dispersed in ethanol at a concentration of ∼30 mg mL^{-1}. QD-LEDs were fabricated on glass substrates coated with ITO with a sheet resistance of ∼20 Ω sq^{-1}. The substrates were cleaned with deionized water, acetone, and isopropanol, consecutively, for 15 min each, and then treated for 15 min with ozone generated by ultraviolet light in air. These substrates were spin-coated with PEDOT:PSS (AI 4083) and baked at 150 °C for 15 min in air. The coated substrates were then transferred to a N_2-filled glovebox for spin-coating of the poly[9,9-dioctylfluorene-co-*N*-[4-(3-methylpropyl)]-diphenylamine] (TFB), $Zn_{1-x}Cd_xS_{1-y}Se_y$/ZnS QD, and ZnO nanoparticle layers. The TFB hole-transport layer was spin-coated using 1.5 wt % in chlorobenzene (2000 rpm for 30 s), followed by baking at 110 °C for 30 min. This was followed by spin-coating of $Zn_{1-x}Cd_xS_{1-y}Se_y$/ZnS QDs (10 mg mL^{-1}, toluene) and ZnO nanoparticles (30 mg mL^{-1}, ethanol) layers followed by baking at 145 °C for 30 min. The spin speed is 1000 rpm for the QD layer and 4000 rpm for the ZnO nanoparticle layer to achieve layer thickness of ∼20 and ∼25 nm, respectively. These multilayer samples were then loaded into a custom high-vacuum deposition chamber (background pressure, $\sim 3 \times 10^{-7}$ Torr) to deposit the top Al cathode (100 nm thick) patterned by an in situ shadow mask to form an active device area of 4 mm^2.

Characterization. Room temperature UV−vis absorption and PL spectra were measured with an Ocean Optics spectrophotometer (mode PC2000-ISA). PL quantum yields (QYs) were determined by comparison of the integrated fluorescence intensity of the QD samples in solution with that of standard of known QYs (LD 423, QY = 68% in ethanol; coumarin 540, QY = 78% in ethanol). All QYs data of QDs and dyes were collected through Ocean Optics USB2000 spectrometer and an Ocean Optics ISP-50-8-I integrating sphere. The optical density (OD) values of the QD samples and organic dyes at the excitation wavelength were set the same in the range of 0.02−0.05. X-ray diffraction (XRD) studies of NCs were carried out with a Philips X′ Pert Pro X-ray diffractometer using Cu−Ka radiation (λ = 1.54 Å). Transmission electron microscopy (TEM) studies were performed using a JEOL JEM-2010 electron microscope operating at 200 kV. Current−luminance−voltage characteristics were measured using an Agilent 4155C semiconductor parameter analyzer with a calibrated Newport silicon diode. The luminance was calibrated using a Minolta luminance meter (LS-100). The electroluminescence spectra were obtained with an Ocean Optics high-resolution spectrometer (HR4000) and a Keithley 2400 power source.

RESULTS AND DISCUSSION

The composition-dependent PL and absorption spectra of $Zn_{0.5}Cd_{0.5}S_{1-y}Se_y$ core QDs (Figure 1) were used for representing the spectra of the various composition ratios of $Zn_{1-x}Cd_xS_{1-y}Se_y$ core QDs. $Zn_{0.5}Cd_{0.5}S_{1-y}Se_y$ QDs recorded in the composition of the molar ratio of S and Se range from 9: 1 to 1:9, and the PL peak shifts from 460, 474, 486, and 512 to 538 nm, respectively. The photoluminescence of $Zn_{0.5}Cd_{0.5}S_{1-y}Se_y$ QDs redshift with the increase of the amount of Se due to the narrower band gap of $Zn_{0.5}Cd_{0.5}Se$ than of $Zn_{0.5}Cd_{0.5}S$. Powder X-ray diffraction (XRD) patterns of the typical $Zn_{0.5}Cd_{0.5}S_{1-y}Se_y$ core QDs (Supporting Information Figure S1) reveal that they all have a zinc blende cubic crystal structure. The diffraction peaks were apparently located between those of the bulk CdSe and ZnS composites and gradually shifted toward smaller angles as the S:Se molar ratio changed from 9:1 to 1:9, indicating increased lattice constants of the QDs with gradual substitution of S atoms with the bigger and heavier Se atoms, which is in accordance with Vegard's law.[28,29] Furthermore, by adjusting the relative amounts of the four elements, the band gaps of the ZnCdSSe QDs can be continuously tuned from 450 to 550 nm. Figure 1b shows PL data for a series of ZnCdSSe QDs with PL peaks at 460

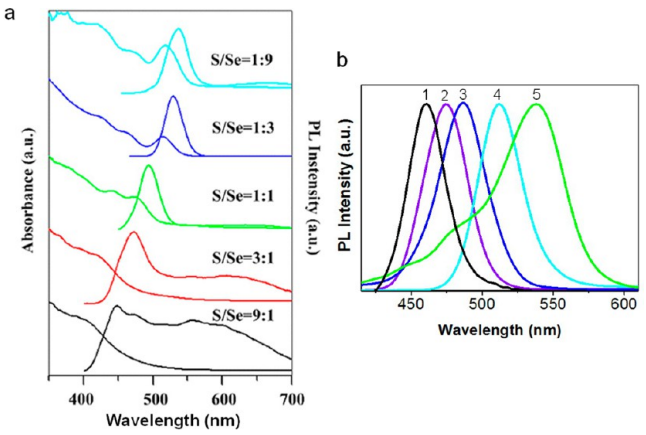

Figure 1. (a) Absorption and photoluminescence spectra of $Zn_{0.5}Cd_{0.5}S_{1-y}Se_y$ QDs with a constant Zn:Cd molar ratios of 1:1 along with different S:Se molar ratios for 9:1, 3:1, 1:1, 1:3, and 1:9, respectively. (b) Composition-dependent band-edge emission of ZnCdSSe QDs. (1) Zn:Cd:S:Se = 9:1:9:1; (2) Zn:Cd:S:Se = 4:1:4:1; (3) Zn:Cd:S:Se = 7:3:6:4; (4) Zn:Cd:S:Se = 3:2:2:3; and (5) Zn:Cd:S:Se = 1:2:1:2.

(9:1:9:1), 474 (4:1:4:1), 486 (7:3:6:4), 512 (3:2:2:3), and 550 nm (1:2:1:2), respectively.

It is well-known that ZnS is the most widely used shell material for core/shell structures, because its relatively wide band gap can effectively confine both the electrons and the holes to the core region and thus improve the PL QYs and stability.[24] Figure 2 shows the absorption and PL spectra of the

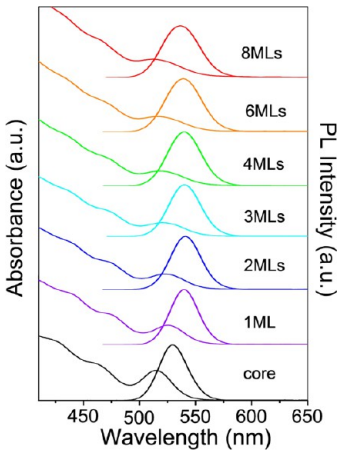

Figure 2. Evolution of the absorption and PL spectra upon consecutive growth of $Zn_{0.5}Cd_{0.5}S_{0.25}Se_{0.75}$/ZnS core/shell QDs.

core/shell QDs from a typical reaction. The result indicates that such ZnS layers indeed enhanced both QY and stability of alloyed $Zn_{1-x}Cd_xS_{1-y}Se_y$ QDs. The highest QYs of these as-synthesized $Zn_{0.5}Cd_{0.5}S_{0.25}Se_{0.75}$/ZnS core/shell QDs could reach 75%. High temperature is needed in our synthesis. The relatively high reaction temperature not only promote the Zn ion for growth ZnS shell but also diffuse the Zn ion into the surface of $Zn_{1-x}Cd_xS_{1-y}Se_y$ core that forms a consecutive change of lattice parameters from core to shells without the formation of structural defects. Figure 2 also shows that during the first monolayer (ML) of the shell growth from the $Zn_{0.5}Cd_{0.5}S_{0.25}Se_{0.75}$ core QDs, the absorption and PL spectra shifted to the red due to the larger extension of the electronic wave function leaking out into the shell material.[30] During the subsequent shell growth, the absorption and PL-spectra slightly shifted to the blue, which was observed by Xie and co-workers,[31] who discovered that the blue-shift was only happened when the particles are covered with additional ZnS. This phenomenon was ascribed to the fact that the Zn-atoms diffuse into the Cd-rich regions of the shell at high temperature, thus increasing the band-offset of the shell and hence the effective confinement.[31,32] With the shell growth, the fwhm (full width at half-maximum) increases from 29 to 39 nm. To prove the high stability of as-synthesized $Zn_{0.5}Cd_{0.5}S_{0.25}Se_{0.75}$/ZnS core/shell QDs, ligand loss tests were adopted. It is clearly shown that the QYs of core−shell QDs do not show any decline upon many times of precipitation and redispersion in hexanes (Supporting Information Figure S2).

To further characterize the evolution of structures of $Zn_{0.5}Cd_{0.5}S_{0.25}Se_{0.75}$/ZnS core/shell QDs, we also verified the crystallographic properties by XRD (Figure 3). The XRD

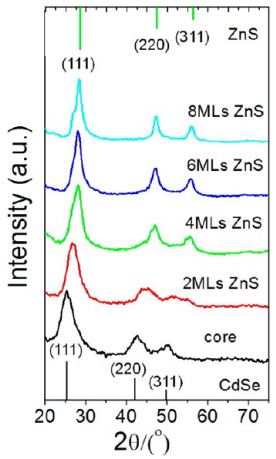

Figure 3. Powder XRD patterns of $Zn_{0.5}Cd_{0.5}S_{0.25}Se_{0.75}$ cores and core/shell QDs with different monolayers (MLs) of ZnS shell. For comparison, the standard powder diffraction patterns of cubic CdSe and ZnS bulk crystals are provided.

patterns of bulk cubic CdSe and ZnS are shown at the bottom and top of Figure 3, respectively. The XRD pattern of the $Zn_{0.5}Cd_{0.5}S_{0.25}Se_{0.75}$ shows three obvious diffraction peaks located at 25.5, 42.7, and 50.2 degrees corresponding to the (111), (220), and (311) planes, respectively, which lie between the bulk CdSe and ZnS of zinc blende structure. It is also clearly shown that XRD peaks get narrower along with the increase of shell thicknesses, which indicates the increase of the QDs' sizes. An obvious peak shift to larger reflection angle positions has been observed when ZnS shells were grown and all samples still kept zinc blende structures. For better comparison, TEM images of the core QDs and several core/shell QDs with different shell thicknesses are shown in Figure 4a−e. All the TEM images show nearly monodisperse spherical QDs with average diameters of 4.3 (b), 6.2 (c), 7.0 (d), and 7.8 nm (e) after shells were grown onto the original $Zn_{0.5}Cd_{0.5}S_{0.25}Se_{0.75}$ core QDs with a diameter of 3.5 nm (a). The corresponding HRTEM images of $Zn_{0.5}Cd_{0.5}S_{0.25}Se_{0.75}$ cores and core/shell QDs are shown in Figure 4a1−e1. As shown in the HRTEM image of $Zn_{0.5}Cd_{0.5}S_{1-x}Se_x$ core QDs, the lattice spacing of the (111) planes is 0.35 nm, which is bigger than that of zinc blende ZnS (0.313 nm) and smaller than that of zinc blende CdSe (0.351 nm). With the increase of

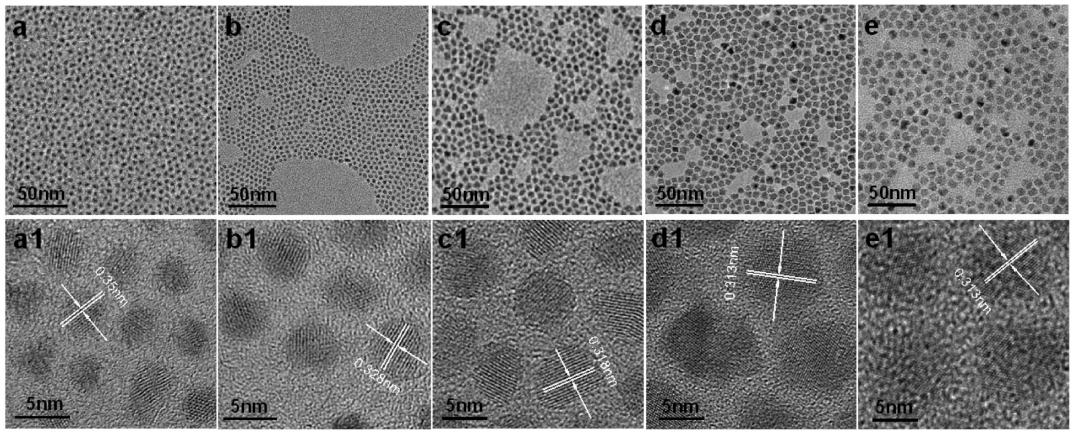

Figure 4. TEM and HRTEM (inset) images of the $Zn_{0.5}Cd_{0.5}S_{0.25}Se_{0.75}$ cores and core/shell QDs obtained under typical reaction conditions: (a) TEM images of $Zn_{0.5}Cd_{0.5}S_{0.25}Se_{0.75}$ cores; (b) part a plus two monolayers of ZnS; (c) part b plus two monolayers of ZnS; (d) part c plus two monolayers of ZnS; (e) part d plus two monolayers of ZnS. (a1–e1): Corresponding HRTEM of parts a–e.

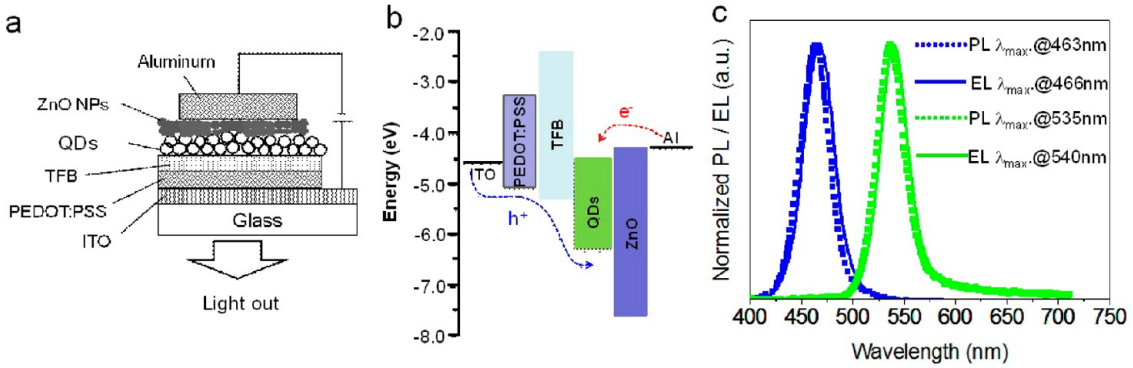

Figure 5. (a) Schematic of layers in the device structure. (b) Energy level diagram for the various layers. (c) Normalized photoluminescence spectra (dashed lines) and EL (solid lines) spectra of blue–green QD-LEDs.

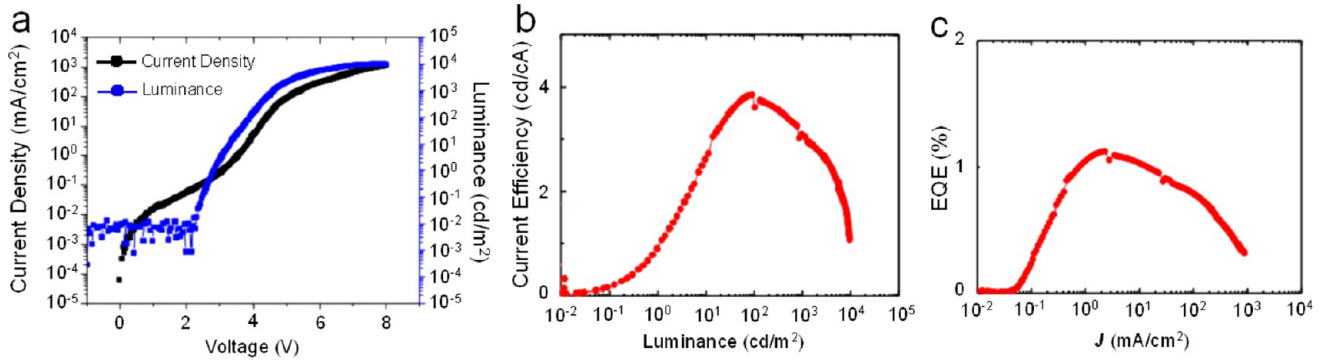

Figure 6. Electroluminescence performance of QD-LEDs with green emission: (a) current–density (J) and luminance (L) versus driving voltage (V); (b) current efficiency versus luminance; (c) external quantum efficiency (EQE) versus current–density.

shell thickness, the lattice parameters decrease gradually toward 0.313 nm, which is consistent with that of zinc blende ZnS. The consecutive change of the lattice parameters can effectively reduce the structural defects and improve the PL QYs.

On the basis of this "green" and efficient synthesis method, we further explored the potential application of $Zn_{1-x}Cd_xS_{1-y}Se_y$/ZnS (x = 0.2, y = 0.1 for blue and x = 0.6, y = 0.5 for green) core/shell QDs as emitters in blue–green LEDs. The structure of the QD-LEDs is schematically shown in Figure 5a, the QD-LEDs were fabricated with layers of indium tin oxide (ITO)/poly(ethylenedioxythiophene):polystyrene sulfonate (PEDOT:PSS) (40 nm)/poly[9,9-dioctylfluorene-co-*N*-[4-(3-methylpropyl)]-diphenylamine] (TFB) (30 nm)/$Zn_{1-x}Cd_xS_{1-y}Se_y$/ZnS core/shell QDs (20 nm)/ZnO NPs (25 nm)/Al to confine exciton formation within the QD layer. TFB and ZnO layers were chosen as the hole-transporting and the electron-transporting layers, respectively, because of their high hole (electron) mobility with effective electron-(hole-)blocking properties. Except for the Al cathode, which was deposited through vacuum thermal evaporation, all the active layers were spin-coated on top of ITO sequentially. Previous research results have indicated the solvent orthogonality in such multilayer structure, which can successfully avoid compromising the integrity of the underlying layers while depositing the

dx.doi.org/10.1021/am400433y | ACS Appl. Mater. Interfaces 2013, 5, 4260–4265

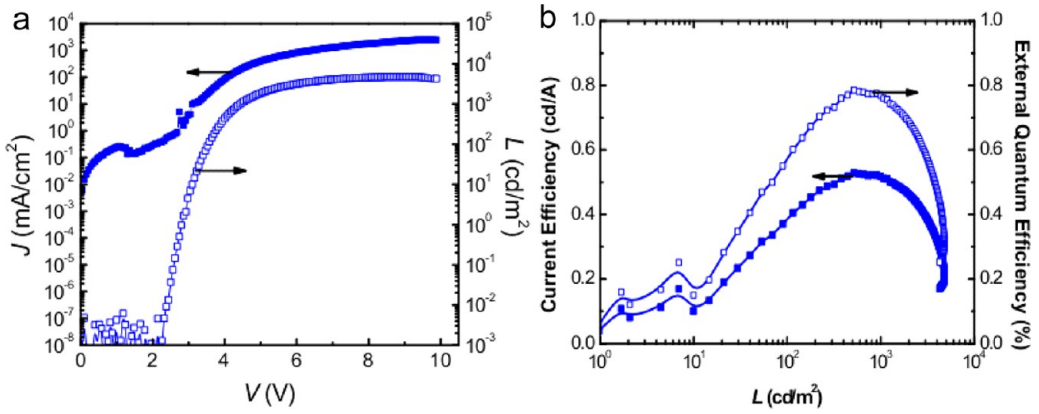

Figure 7. Electroluminescence performance of QD-LED with blue emission: (a) current−density (J) and luminance (L) versus driving voltage (V); (b) current efficiency and external quantum efficiency versus luminance.

overlayers.[11] The schematic energy level diagram (Figure 5b) shows that the ZnO nanoparticle layer not only provides efficient electron injection from the Al cathode into $Zn_{1-x}Cd_xS_{1-y}Se_y$/ZnS QDs but also helps to confine holes within the QD layer due to the valence band offset at the QD/ZnO nanoparticle interface, leading to an improved charge recombination efficiency.[11] Figure 5c shows the PL spectra of $Zn_{1-x}Cd_xS_{1-y}Se_y$/ZnS core/shell QDs and the electroluminescence (EL) spectra of the corresponding QD-LEDs. The blue−green LEDs have EL peaks at wavelength of 466 nm, and 540 nm and all QD-LEDs exhibit EL spectra with a narrow spectral bandwidth (fwhm <50 nm) at a slightly red-shifted wavelength compared with the PL spectra. Most of the emission originates from the $Zn_{1-x}Cd_xS_{1-y}Se_y$/ZnS QDs (99% of the total EL emission). No noticeable parasitic emission from adjacent organic layers (i.e., TFB) has been observed during device operation, which supports the good exciton confinement within the QD layer.

Figure 6a−c are the current density−luminance−voltage (J−L−V) characteristics, current efficiency, and EQE curves for the green QD-LEDs. The green QD-LEDs (EL = 540 nm) typically exhibit the following device characteristics: with the lowest turn on voltage of 2.1 V, highest external quantum efficiency of 1.2% at a current density of 50 mA/cm^2, and maximum brightness above 10 000 cd/m^2 which is lower than previously reported.[11,13,15] But, the blue QD-LED (EL = 466 nm) based on our $Zn_{1-x}Cd_xS_{1-y}Se_y$/ZnS (x = 0.2, y = 0.1) core/shell QDs shows an unprecedentedly high brightness over 4700 cd/m^2 (Fgiure 7a) which is the highest value ever reported for QD-based light-emitting diodes.[11−15] The significant improvement compared to previous reports due to the high QYs of the $Zn_{1-x}Cd_xS_{1-y}Se_y$/ZnS core/shell QDs and the excellent structure of QD-LED. In this structure the injection of electrons and holes into $Zn_{1-x}Cd_xS_{1-y}Se_y$/ZnS core/shell QDs enables the balanced exciton formation and efficient exciton recombination within QD active layers and leads to high efficiency and brightness. The turn-on voltages (driving voltage corresponding to a luminance of 1 cd/m^2), peak luminous efficiency, and peak external quantum efficiency were 2.4 V, 0.52 cd/A, and 0.8% for our blue QD-LED (Figure 7a and b). These results indicate that the $Zn_{1-x}Cd_xS_{1-y}Se_y$/ZnS core/shell QDs may be more suitable for making blue QD-LED just as CdSe/ZnS QDs are more suitable for the production of green QD-LED.[11,15]

CONCLUSIONS

In summary, we have synthesized nearly monodisperse $Zn_{1-x}Cd_xS_{1-y}Se_y$ cores and high quality blue−green fluorescent $Zn_{1-x}Cd_xS_{1-y}Se_y$/ZnS core/shell QDs with a "green" and simple method. The PL QYs of these core/shell QDs reached 75% and their FWHMs were kept below 40 nm. The QD-LEDs fabricated using $Zn_{1-x}Cd_xS_{1-y}Se_y$/ZnS core/shell QDs as emitters display high external quantum efficiency (0.8), and high maximum luminance values (4700 cd/m^2) which is the highest value in blue area ever and comparable to the brightness of the best QD-based LEDs. These results suggest that $Zn_{1-x}Cd_xS_{1-y}Se_y$/ZnS QD-LEDs will be promising for successful realization of high bright and efficient blue−green QD-LEDs and therefore represent a step toward to the realization of QD-based full-color displays or white LEDs.

ASSOCIATED CONTENT

Supporting Information

XRD of ZnCdSSe nanocrystals and PL and QY of ZnCdSSe/ZnS core/shell nanocrystals. This material is available free of charge via the Internet at http://pubs.acs.org.

AUTHOR INFORMATION

Corresponding Author

*E-mail: lsli@henu.edu.cn (L.S.L.), ying.zheng@nanophotonica.com (Y.Z.).

Author Contributions

§H.S. and S.W. contributed equally to this paper.

Notes

The authors declare no competing financial interest.

ACKNOWLEDGMENTS

This work was financially supported by the research project of the National Natural Science Foundation of China (21071041 and 21201055), Program for Changjiang Scholars and Innovative Research Team in University, (No. PCS IRT1126), and Program for New Century Excellent Talents in University of Chinese Ministry of Education (NCET-09-0119).

REFERENCES

(1) Colvin, V. L.; Schlamp, M. C.; Alivisatos, A. P. *Nature* **1994**, *370*, 354.

(2) Coe, S.; Woo, W. K.; Bawendi, M. G; Bulović, V. *Nature* **2002**, *420*, 800.

(3) Steckel, J. S.; Snee, P.; Coe, S.; Zimmer, J. P.; Halpert, J. E.; Anikeeva, P.; Kim, L.; Bulović, V.; Bawendi, M. G. *Angew. Chem., Int. Ed.* **2006**, *45*, 5796.
(4) Kim, L.; Anikeeva, P. O.; Coe, S.; Steckel, J. S.; Bawendi, M. G.; Bulović, V. *Nano Lett.* **2008**, *8*, 4513.
(5) Sun, Q.; Wang, Y. A.; Li, L. S.; Wang, D.; Zhu, T.; Xu, J.; Yang, C.; Li, Y. *Nat. Photon.* **2007**, *1*, 717.
(6) Shirasaki, Y.; Supran, G. J.; Bawendi, M. G; Bulović, V. *Nat. Photon.* **2013**, *7*, 13.
(7) Cho, K.-S.; Lee, E. K.; Joo, W.-J.; Jang, E.; Kim, T.-H.; Lee, S. J.; Kwon, S.-J.; Han, J. Y.; Kim, B.-K.; Choi, B. L.; Kim, J. M. *Nat. Photon.* **2009**, *3*, 341.
(8) Kwak, J.; Bae, W. K.; Zorn, M.; Woo, H.; Yoon, H.; Lim, J.; Kang, S. W.; Weber, S.; Butt, H.-J.; Zentel, R.; Lee, S.; Char, K.; Lee, C. *Adv. Mater.* **2009**, *21*, 5022.
(9) Peng, H.; Kang, C.; Liang, M.; Chen, C.; Demchenko, A.; Chen, C.; Chou, P. *ACS Appl. Mater. Interfaces* **2011**, *3*, 1713.
(10) Pal, B. N.; Ghosh, Y.; Brovelli, S.; Laocharoensuk, R.; Klimov, V. I.; Hollingsworth, J. A.; Htoon, H. *Nano Lett.* **2012**, *12*, 331.
(11) Qian, L.; Zheng, Y.; Xue, J.; Holloway, P. H. *Nat. Photon.* **2011**, *5*, 543.
(12) Bae, W. K.; Kwak, J.; Lim, J.; Lee, D.; Nam, M. K.; Char, K.; Lee, C.; Lee, S. *Nanotechnology* **2009**, *20*, 075202.
(13) Bae, W. K.; Kwak, J.; Park, J. W.; Char, K.; Lee, C.; Lee, S. *Adv. Mater.* **2009**, *21*, 1690.
(14) Kim, T.-H.; Cho, K.-S.; Lee, E. K.; Lee, S. J.; Chae, J.; Kim, J. W.; Kim, D. H.; Kwon, J.-Y.; Amaratunga, G.; Lee, S. Y.; Choi, B. L.; Kuk, Y.; Kim, J. M.; Kim, K. *Nat. Photon.* **2011**, *5*, 176.
(15) Kwak, J.; Bae, W. K.; Lee, D.; Park, I.; Lim, J.; Park, M.; Cho, H.; Woo, H.; Yoon, D. Y.; Char, K.; Lee, S.; Lee, C. *Nano Lett.* **2012**, *12*, 2362.
(16) Nevins, J.; Coughlin, K.; Watson, D. *ACS Appl. Mater. Interfaces* **2011**, *3*, 4242.
(17) Wu, P.; Dai, Y.; Sun, T.; Ye, Y.; Meng, H.; Fang, X.; Yu, B.; Dai, L. *ACS Appl. Mater. Interfaces* **2011**, *3*, 1859.
(18) Peng, X.; Manna, L.; Yang, W.; Wickham, J.; Scher, E.; Kadavanich, A.; Alivisatos, A. P. *Nature* **2000**, *404*, 59.
(19) Wang, W.; Germanenko, I.; El-Shall, M. S. *Chem. Mater.* **2002**, *14*, 3028.
(20) Zhong, X.; Feng, Y.; Knoll, W.; Han, M. *J. Am. Chem. Soc.* **2006**, *128*, 9002.
(21) Zhong, X.; Feng, Y.; Zhang, Y.; Gu, Z.; Zou, L. *Nanotechnology* **2007**, *18*, 385606.
(22) Zhong, X.; Han, M.; Dong, Z.; White, T. J.; Knoll, W. *J. Am. Chem. Soc.* **2003**, *125*, 8589.
(23) Shen, H.; Wang, H.; Zhou, C.; Niu, J.; Yuan, H.; Ma, L.; Li, L. S. *Dalton Trans.* **2011**, *40*, 9180.
(24) Shen, H.; Zhou, C.; Xu, S.; Yu, C.; Wang, H.; Chen, X.; Li, L. S. *J. Mater. Chem.* **2011**, *21*, 6046.
(25) Deng, Z.; Yan, H.; Liu, Y. *J. Am. Chem. Soc.* **2009**, *131*, 17744.
(26) Xu, S.; Shen, H.; Zhou, C.; Yuan, H.; Liu, C.; Wang, H.; Ma, L.; Li, L. S. *J. Phys. Chem. C.* **2011**, *115*, 20876.
(27) Shen, H.; Wang, H.; Tang, Z.; Niu, J.; Lou, S.; Du, Z.; Li, L. S. *CrystEngComm* **2009**, *11*, 1733.
(28) Deng, Z.; Cao, L.; Tang, F.; Zou, B. *J. Phys. Chem. B* **2005**, *109*, 16671.
(29) Deng, Z.; Mansuripur, M.; Muscat, A. J. *Nano Lett.* **2009**, *9*, 2015.
(30) Schoos, D.; Mews, A.; Eychmüller, A.; Weller, H. *Phys. Rev. B* **1994**, *49*, 17072.
(31) Xie, R.; Kolb, U.; Li, J.; Basché, T.; Mews, A. *J. Am. Chem. Soc.* **2005**, *127*, 7480.
(32) Zhong, X.; Feng, Y.; Knoll, W.; Han, M. *J. Am. Chem. Soc.* **2003**, *125*, 13559.